[Geochemistry, Geophysics, Geosystems]

Supporting Information for

Comment on "Influence of data filters on the position and precision of paleomagnetic poles: what is the optimal sampling strategy? " by Gerritsen et al. (2022)

Pierrick Roperch

Géosciences Rennes

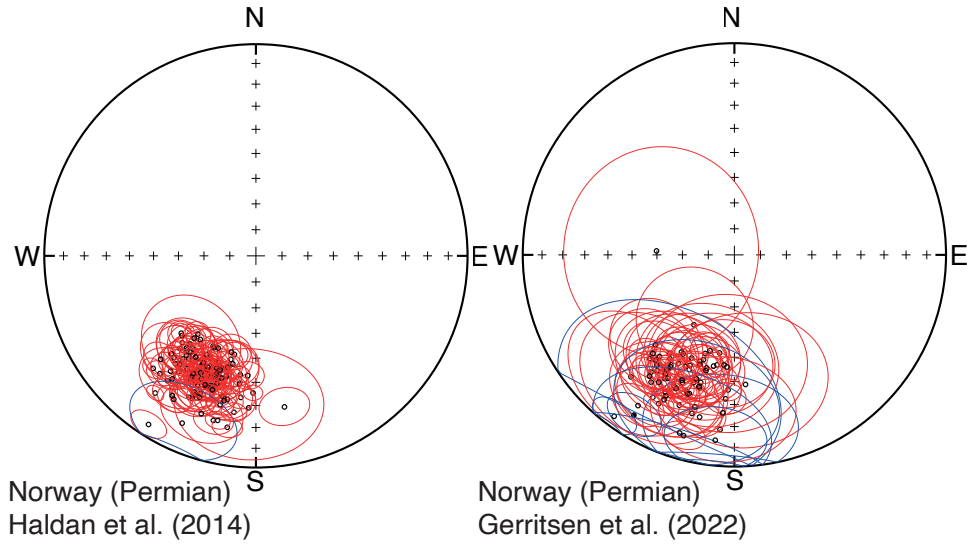**Contents of this file**

Figures S1 to S11

Figure S1.

Equal-area projections of site-mean directions from the original paper of Haldan et al. (2014) and the directions calculated from the directions in the supplementary data of Gerritsen et al.
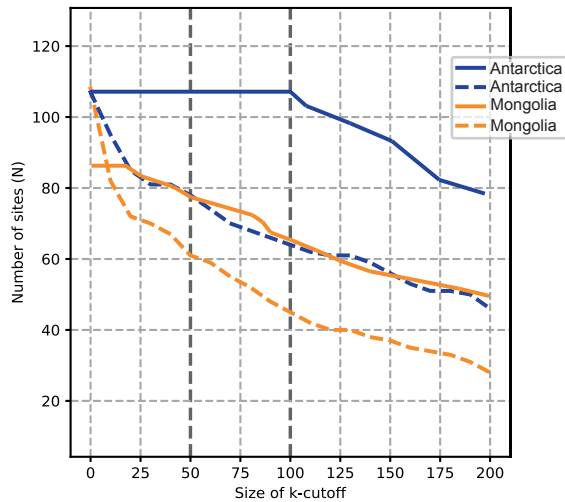

Figure S2.

Comparison of the number of sites above a certain k value as shown in Figure 4a of Gerritsen et al. (2022). The dashed line is with the selected GVH data. Solid line from Antarctica is from the original data of Asefaw et al. where all sites have k values greater than 100. The solid line from Mongolia corresponds to the present analysis of the original paleomagnetic data downloaded from Magic. 20 sites without well-defined characteristic directions are rejected.
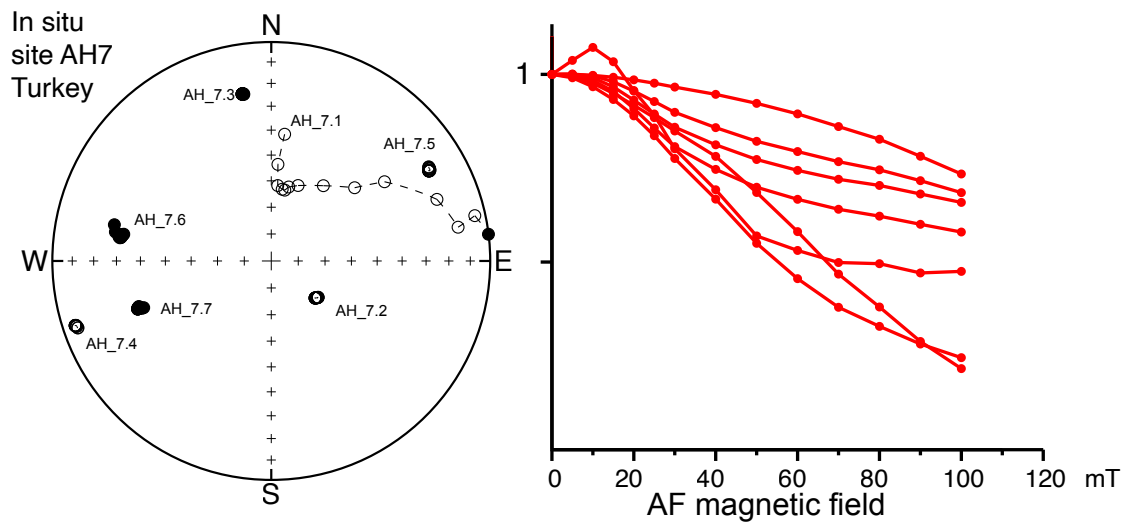
Figure S3.

Paleomagnetic results at site AH7 from the Turkey database. Left) Equal-area plot of the directions for the seven samples during Alternating field demagnetization. The paleomagnetic data are clearly scattered between samples but with a stable ChRM for 6 out of 7 samples and high medium destructive field values.
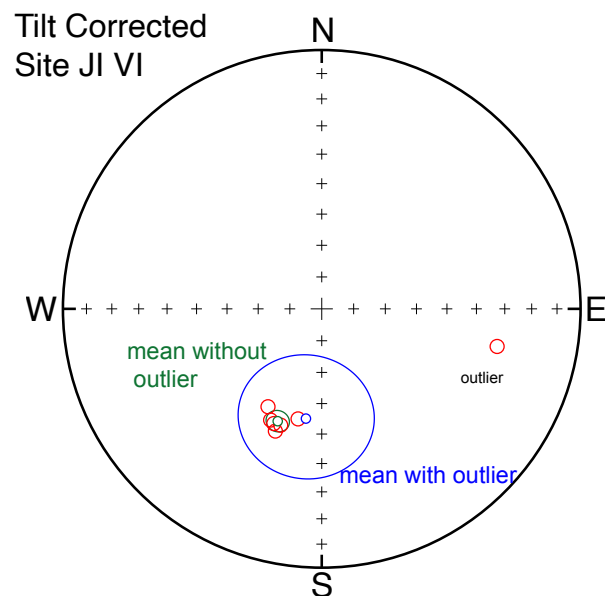

Figure S4.

Stereonet projection of ChRMs components (red circles) for site JI VI (Mongolia). There is clearly an outlier. The mean was calculated without (green circle) or with the outlier (blue circle) as done by Gerritsen et al. (2022).
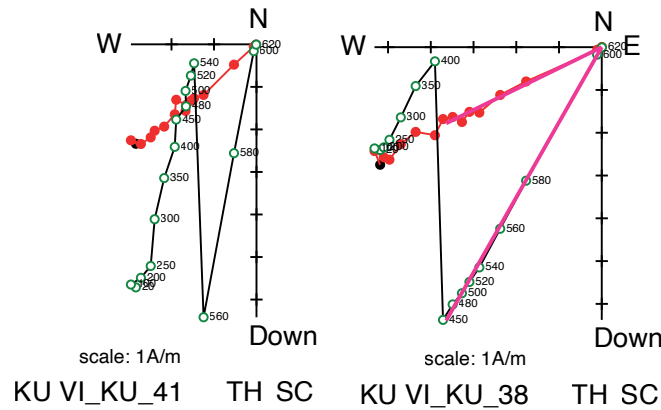
Figure S5.

Orthogonal plot of thermal demagnetization in sample coordinate. Examples of problems in measurements with a jump in the Z component possibly due to either problems while uploading data in the database or in the laboratory. All the samples from the site(KU VI, Mongolia) are affected by this problem but not at the same temperature. The ChRM was calculated using the high temperature data.
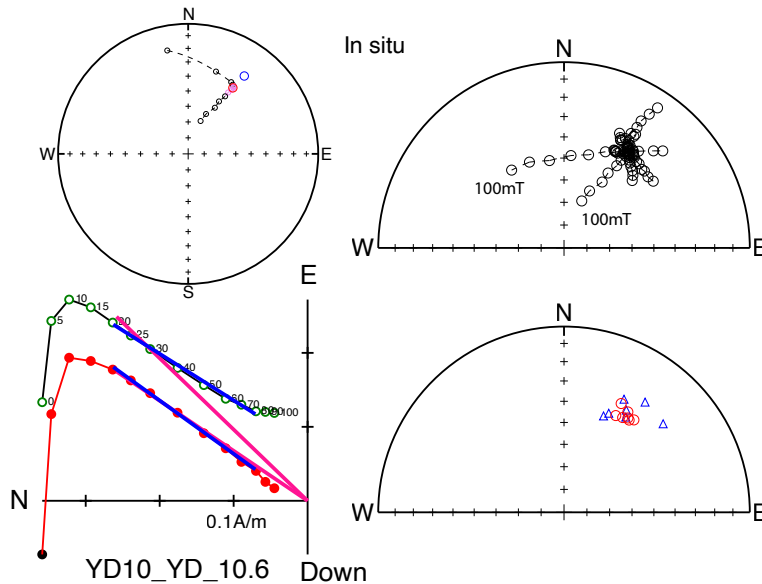

Figure S6.

Examples of AF demagnetization with possible deflection of the ChRM due to GRM acquisition. Left) demagnetization data for sample YD10.6 with the ChRM calculated by forcing the calculation of the ChRM though the origin (red line) or without (blue line). Upper right) Plot of the demagnetization data above 20mT for all samples from the site. Bottom right) ChRM directions for the seven samples (red circles forcing to the origin and blue triangles (GVH)
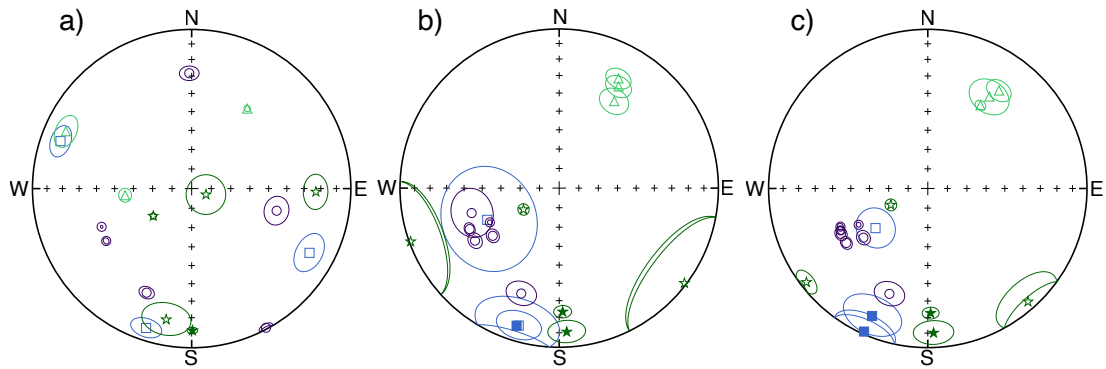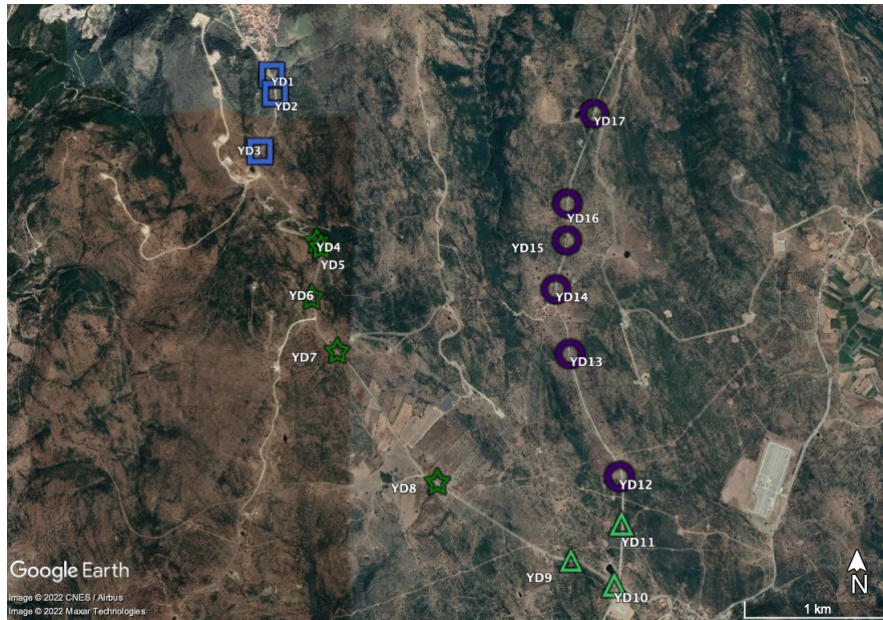
Figure S7.

Top) Google Earth image with the paleomagnetic sampling of the Yuntdag area (Turkey) from van Hinsbergen et al. (2010). a) Stereonet of the ChRM site-mean directions reported by van Hinsbergen et al. in their original publication. b) Stereonet of the site-mean directions calculated from ChRMs defined by GVH. c) Stereonet of the ChRMs determined in this study. There are slight differences between the site-mean directions determined in the present study (c) and those in GVH (b) due to the inclusion of outliers and deflection of the ChRMs by GRMs. But several of the site-mean directions calculated in the original publication, especially using great circles are unreliable.
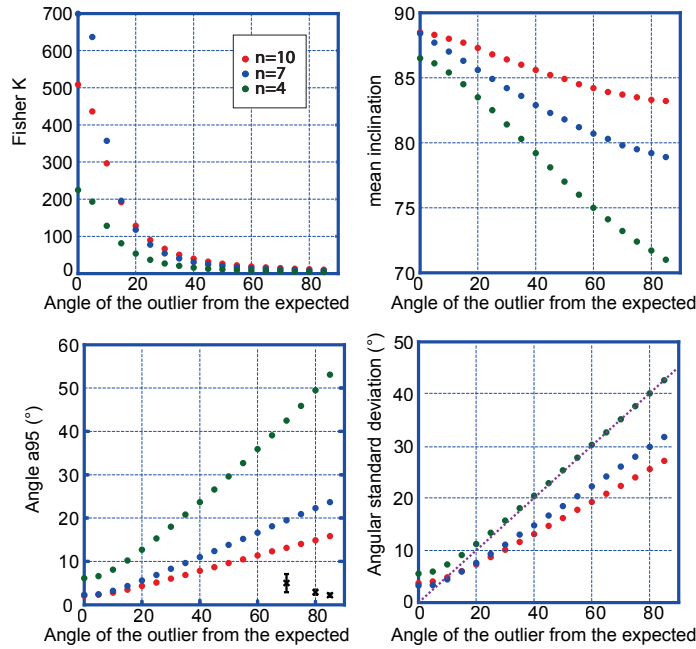
5

Figure S8.

Effect of an outlier in the calculation of a site-mean direction calculated with 4, 7 or 10 samples. A Fisher population was generated with an initial Fisher parameter k of 500 around a direction with an inclination of 90°. The outlier was progressively shifted from the mean by steps of 5° and Fisher statistics were calculated.
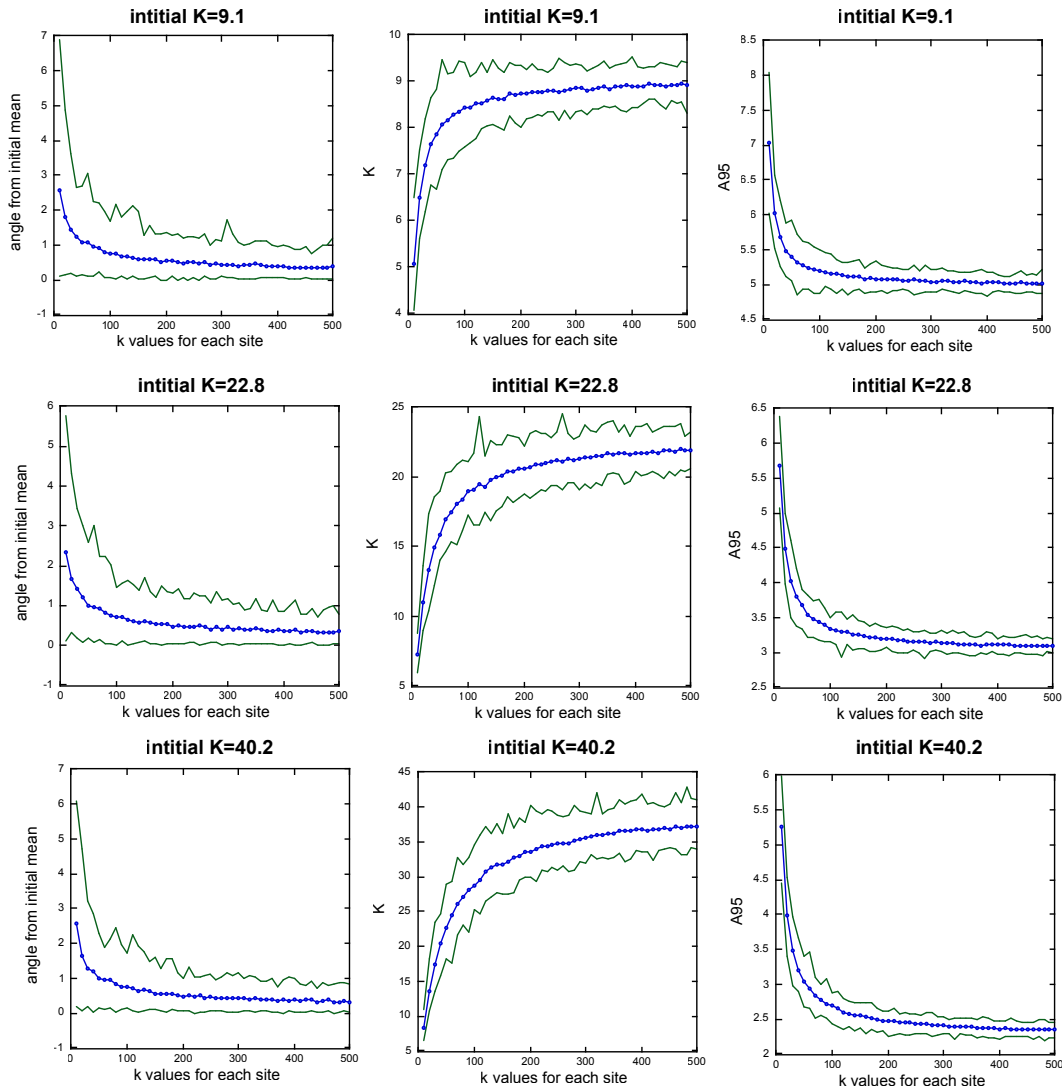
Figure S9.

Comparison of the effect of selecting one sample per site in the calculation of the mean direction for three initial populations of 100 directions with an initial Fisherian distribution with k of 9.1, 22.8 and 40.2. For each site one direction was simulated from a Fisherian population of k values ranging from 10 to 500. The process was repeated 100 times to establish the mean (blue circles) and the min and max values. When all sites have a Fisher parameter greater than 100, the angles of the mean direction from the initial mean direction are on average at less than 1° from the mean. This figure illustrates the between site scatter control on the statistical characteristics over the within-site scatter except when an unusual large number of sites have directions defined by low-k values
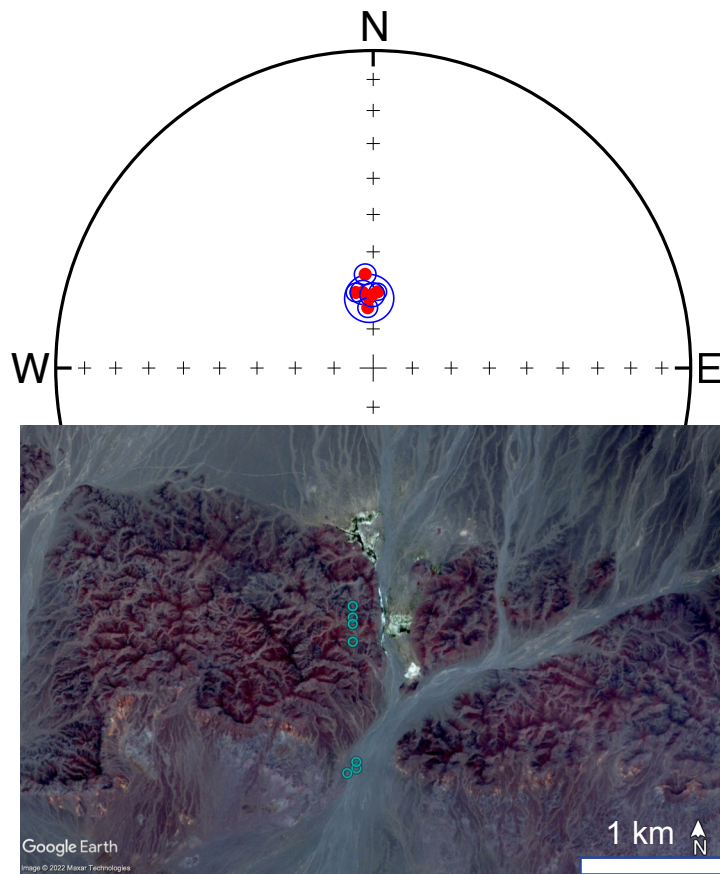
Figure S10.

Paleomagnetic directions from seven nearby sites apparently drilled in the same volcanic unit. Top) Stereograph showing the tight grouping of the seven site-mean directions. Bottom, Google earth image showing the location of the sites. All sites are drilled over a distance of about 1 km at an elevation of ~1450 ±10m suggesting that it is a single flat lying volcanic unit.
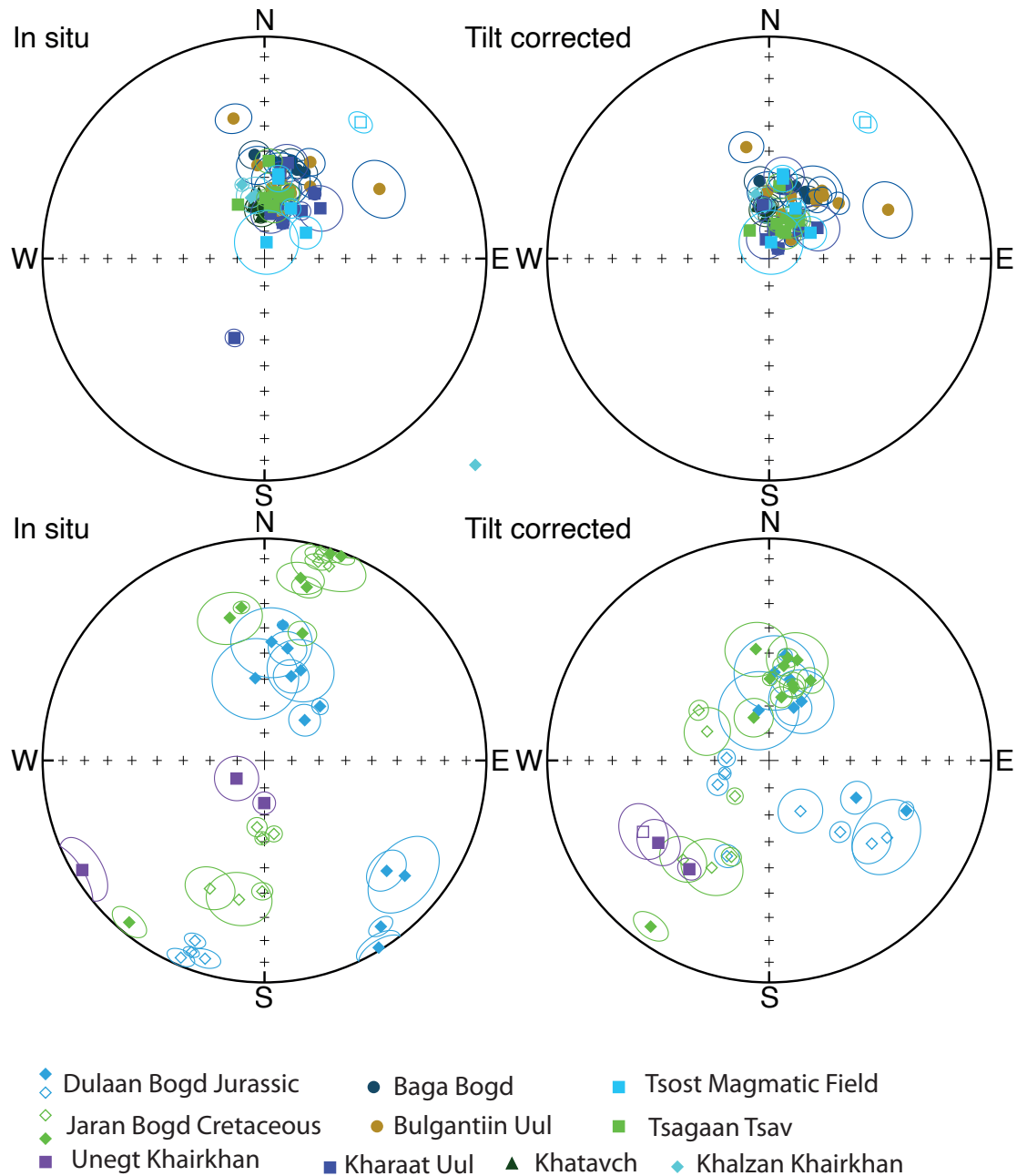
Figure S11.

Stereographic projections of Site-mean directions calculated from the database from Mongolia in in situ (left) and after bedding correction (right). The upper stereonets correspond to areas with mostly flat lying bedding. The lowermost stereonets correspond to areas with more complex bedding and these areas record the farthest site-mean directions from the mean. Most of the outliers may be due to incorrect bedding corrections rather than secular variation.